NJC

PAPER

View Article Online
View Journal | View Issue

Cite this: *New J. Chem.*, 2019, 43, 17711

Synthesis, structure and biological evaluation of mixed ligand oxidovanadium(IV) complexes incorporating 2-(arylazo)phenolates†

Sudhir Lima,[a] Atanu Banerjee,[a] Monalisa Mohanty,[a] Gurunath Sahu,[a] Chahat Kausar,[b] Samir Kumar Patra,[b] Eugenio Garribba,[c] Werner Kaminsky[d] and Rupam Dinda *[a]

[VO(acac)$_2$] was used as a metal precursor to synthesize a series of mixed ligand oxidovanadium(IV) complexes [$V^{IV}O(L^{1-4})(L^{NN})$] (**1–5**) with tridentate ONO donor arylazo ligands (H_2L^{1-4}) (where H_2L^1 = 1-(2-hydroxyphenyl)diazenyl)naphthane-2-ol, H_2L^2 = 1-(2-hydroxy-4-methylphenyl)diazenyl)naphthane-2-ol, H_2L^3 = 1-(2-hydroxy-4-nitrophenyl)diazenyl)naphthane-2-ol and H_2L^4 = 1-(2-hydroxy-4-bromophenyl)diazenyl)naphthane-2-ol) along with an ancillary ligand (L^{NN}), namely 2,2′-bipyridine (bipy) or 1,10-phenanthroline (phen) as a co-ligand. All complexes were characterized by spectroscopic, ESI-MS and X-ray crystallographic techniques, which show their distorted octahedral geometry. The molecular structure shows the presence of a vanadyl group in six-coordinated $V^{IV}N_3O_3$ geometry. The species exhibit quasi-reversible one-electron transfer of $E^c_{1/2}$ value between −1.29 and −1.37 V, while irreversible one-electron oxidation peaks lie in the range 0.37–0.67 V *versus* SCE in acetonitrile solution. All the complexes show DNA binding activity with CT-DNA having binding constant values in the range 7.1×10^3–2.03×10^4 M^{-1}. The interaction of synthesized mixed ligand oxidovanadium(IV) species with bovine serum albumin (BSA) was also studied experimentally, which revealed moderate binding affinity. Further, the antiproliferative activity of **1–5** was examined against A549 (lung cancer) cancer cell lines by MTT assay. The cytotoxicity of the complexes is affected by the various functional groups attached to the arylazo derivative as well as the presence of two different co-ligands and **2** showed considerable antiproliferative activity compared to other chemotherapeutic drugs.

Received 13th April 2019,
Accepted 12th July 2019

DOI: 10.1039/c9nj01910c

rsc.li/njc

Introduction

Designing metal based drugs is an active area of research in medicinal inorganic chemistry to develop alternatives to platinum based anticancer drugs such as cisplatin and its derivatives because of their limitations and disadvantages,[1] underlining the importance to develop non-platinum transition metal complexes as anti-cancer agents for possible therapeutic uses. Therefore, efforts have been made in the last few years to synthesize metal-based drugs specifically considering biocompatibility, toxicity, high pharmacological effect, target-specificity and non-covalent binding with DNA.[2] Further, increasing the capability of metal complexes to interact with DNA can allow us to design new and promising drugs, develop new probes for nucleic acids, allow study of DNA-dependent electron transfer reactions, improve DNA footprinting techniques, and to develop sequence-specific cleaving agents and antitumor drugs.[3] Also, proteins are the most important biomolecules responsible for maintaining normal cell functions. Bovine serum albumin (BSA) is the major soluble protein in blood. It is often used as a target protein molecule because of its medical importance, low cost, easy availability, intrinsic fluorescence emission, and structural homology with human serum albumin (HSA).[4] In addition, it can regulate many physiological processes, such as maintaining the pH level of blood and the osmotic pressure, and has the ability to transport many endogenous and exogenous compounds, for example, fatty acids, steroids, drugs, metal ions and metabolites.[5] Hence, the interactions of transition metal complexes with DNA and BSA are

[a] *Department of Chemistry, National Institute of Technology, Rourkela, 769008, Odisha, India. E-mail: rupamdinda@nitrkl.ac.in*
[b] *Department of Life Science, National Institute of Technology, Rourkela, 769008, Odisha, India*
[c] *Dipartimento di Chimica e Farmacia, Università di Sassari, Via Vienna 2, I-07100 Sassari, Italy*
[d] *Department of Chemistry, University of Washington, Seattle, Washington 98195, USA*

† Electronic supplementary information (ESI) available: Tables S1–S4 and Fig. S1–S14. CCDC 1907844–1907848. For ESI and crystallographic data in CIF or other electronic format see DOI: 10.1039/c9nj01910c

currently key research areas for both inorganic chemists and biochemists.[6a–e]

Among the transition metals, vanadium is an essential trace element in biological systems. It is reported that vanadium can reduce the concentration of cholesterol, triglycerides in blood vessels and is also responsible for the enhancement of oxygen-affinity of hemoglobin and myoglobin.[6f–h] In addition, the coordination chemistry of vanadium compounds is of interest because of its biological properties[7] such as antiproliferative,[7a–d,fg,8] and it is involved in DNA binding[7b–e,9] and photo-induced DNA cleavage[7b–e,10] and exhibits insulin mimetic activity.[7a,f,11] Moreover, vanadium also has the ability to control biological processes such as cellular regulation[12] and many physiological processes such as haloperoxidation,[13–16] phosphorylation,[17] vanadium nitrogenases,[18] and antifungal/antibacterial[7h,19] activities.

On the other hand, the coordination chemistry of the azo (N═N) functionalized ligand is of interest because of its properties as a noninnocent ligand[20] and low-lying azo centered molecular orbital.[21] Furthermore, metal mediated azo ligands have become a focus of attraction because of their π-acidity, metal binding ability, dying and pigmenting behavior, and redox, photo-physical, catalytic and biological properties[22] Also, azo complexes are involved in many biological processes, such as inhibition of DNA, RNA, and protein synthesis, nitrogen fixation, and carcinogenesis.[23] Thus, the synthesis of ligands containing a –N═N– group is an important area of research. Again, ligands based on the pyridine ring, like 2,2′-bipyridine, 2,2′-bipyrimidine, 1,10-phenanthroline, and related terpyridine derivatives are among the most versatile and studied ligands.[24] They easily form complexes with transition metal ions in different oxidation states and many of them have also shown pharmacological activity; for example, anti-ulcer action with Bi^{III},[25] anti-cancer activity with Ru^{III},[26] anti-bacterial and anti-parasitic action with Rh^{II},[27] and possible anti-cancer effects with Pt^{II},[28] Au^{III},[29] Ti^{IV},[30] Pd^{II},[31] and Mn^{II}.[32] Specifically, it was also proven that some $V^{IV}O$ complexes designed with 2,2′-bipyridine, 1,10-phenanthroline and their derivatives are effective as anti-cancer agents,[33] and anti-diabetic drugs[34] and show anti-oxidant action.[35] Keeping all the above results in mind, in this work we focus on the complex formation of 2-arylazo derivatives as main ligands and 2,2′-bipyridine and 1,10-phenanthroline as co-ligands with $V^{IV}O$ ions, whose pharmacological potential is well recognized.[33–36]

Over the last few years, we have been studying the chemistry of oxido and nonoxido vanadium(IV/V) complexes incorporating several O,N[7,37] and O,N,S[7f] donor ligands in relation to their DNA/BSA binding,[7b–e] photoinduced DNA cleavage,[7b–e] and antiproliferative[7a–d,f,g] and insulin mimetic activity.[7a,f] In continuation, herein we have reported the synthesis, characterization and biological evaluation of series of mixed ligand oxidovanadium(IV) complexes $[V^{IV}O(L^{1-4})(L^{NN})]$ (**1–5**) containing tridentate arylazo derivatives as main ligands and bidentate ancillary ligands 2,2′-bipyridine and 1,10-phenanthroline as co-ligands. Complexes (**1–5**) were characterized by using different physicochemical, spectroscopic and single crystal X-ray diffraction techniques. The interactions of these complexes (**1–5**) with CT-DNA and BSA (bovine serum albumin) were studied. In addition, the cytotoxicity of the complexes against A549 cell lines was studied.

Experimental section

General methods and materials

2,2′-Bipyridine (bipy), 1,10-phenanthroline (phen), 2-amino-5-nitrophenol and 2-amino-5-methylphenol were purchased from Sigma-Aldrich, whereas β naphthol was from Merck, 2-aminophenol was from Avra and 2-amino-5-bromophenol was purchased from TCI chemicals and used without further purification. Calf thymus (CT) DNA was purchased from SRL (India) (biochemistry grade). Bovine serum albumin (BSA), DAPI (4,6-diamidino-2-phenylindole dihydrochloride) and propidium iodide were supplied by Sigma Aldrich (USA). Methyl green and ethidium bromide were procured from HiMedia Laboratories. MTT was procured from Spectrochem. A549 (lung cancer) cell line was purchased from NCCS, Pune. The arylazo ligands (H_2L^{1-4})[7g] and the metal precursor $[VO(acac)_2]$[38] were prepared by the reported methods. The syntheses were performed under inert atmosphere using Schlenk techniques. Elemental analyses were carried out on a Vario ELcube CHNS Elemental analyzer. IR spectra were recorded on a PerkinElmer Spectrum RXI spectrophotometer. ^1H and ^{13}C NMR spectra were recorded on a Bruker Ultrashield 400 MHz spectrometer in the presence of $SiMe_4$ as an internal standard. Electronic spectra were recorded on a Shimadzu spectrophotometer (UV-2450). Electrospray ionization mass spectra (ESI-MS) were recorded on a Bruker MAT SSQ 710 spectrometer. Electrochemical data were collected with the help of a CH-Instruments (Model No. CHI6003E) in the presence of acetonitrile as a solvent and TBAP (tetrabutylammonium perchlorate) was used as the supporting electrolyte under inert atmosphere at 298 K by using a Pt working electrode, Pt auxiliary electrode and SCE as a reference electrode, whereas the ferrocene–ferrocenium couple was used as a standard to calibrate the instrument. EPR spectra were recorded at 298 K using an X-band (9.4 GHz) JESFA200 ESR spectrometer equipped with microwave power, 0.998 mW. ^{51}V spin-Hamiltonian parameters (g_{iso} and A_{iso}) were simulated with the WINEPR SimFonia software,[39] taking into account the third-order effects; the ratio Lorentzian/Gaussian was 0.2, linewidth was described through the m_i dependent equation $a + bm_i + cm_i^2$, where m_i is the nuclear magnetic quantum number and a, b and c are three numerical coefficients ($a = 30$, $b = -2$ and $c = 2$ for the solid state spectra, and a between 90 and 150, b between −1 and −12 and c between 0 and 10 for the solution spectra). A Fluoromax 4P spectrofluorometer (Horiba Jobin Mayer, USA) was used for the competitive DNA binding analysis. We have performed NMR and UV-vis in 100% DMSO, whereas biological assays were in less than 2% DMSO as solvent. But, for the other two experiments using EPR and cyclic voltammetry we have used DCM and acetonitrile, respectively, because these two experiments give better results in those solvents as we observed earlier.[7a,f,h,37b,c] Again, when using EPR spectra to characterize the structures of complexes, it is better to use a

non-coordinating solvent such as DCM to maintain their identity and not to allow them to undergo dissociation/isomerization.

Synthesis of ligands (H_2L^{1-4})

The ligands H_2L^{1-4} were prepared *via* a two-step process. In the first step an aromatic diazonium ion was prepared from a substituted aminophenol derivative. The next step is coupling of the diazotized substituted aminophenol with β naphthol.[7g] The resulting solid compounds were collected by filtration, washed thoroughly with cold water and finally dried over fused $CaCl_2$. Synthesized ligands have been characterized through elemental analyses, NMR (^{1}H and ^{13}C) and IR spectroscopy.

H_2L^1. Yield: 62%. Anal. calcd for $C_{16}H_{12}N_2O_2$: C, 72.72; H, 4.58; N, 10.60. Found: C, 72.69; H, 4.50; N, 10.69. IR (KBr pellet, cm^{-1}): 3448 ν(O–H); 1545 ν(N=N). ^{1}H NMR (400 MHz, DMSO-d_6): δ 9.73 (s, 1H, OH), 8.50–6.85 (m, 10H, aromatic). ^{13}C NMR (100 MHz, DMSO-d_6): δ 137.2–116.1 (16C, aromatic).

H_2L^2. Yield: 64%. Anal. calcd for $C_{17}H_{14}N_2O_2$: C, 73.37; H, 5.07; N, 10.07. Found: C, 73.37; H, 5.09; N, 10.09. IR (KBr pellet, cm^{-1}): 3382 ν(O–H); 1552 ν(N=N). ^{1}H NMR (400 MHz, DMSO-d_6): δ 8.81 (s, 1H, OH), 7.65–6.47 (m, 9H, aromatic), 2.20 (s, 3H, CH_3). ^{13}C NMR (100 MHz, DMSO-d_6): δ 138.69–118.01 (16C, aromatic), 21.66 (–CH_3).

H_2L^3. Yield: 64%. Anal. calcd for $C_{16}H_{11}N_3O_4$: C, 62.14; H, 3.58; N, 13.59. Found: C, 62.10; H, 3.61; N, 13.56. IR (KBr pellet, cm^{-1}): 3389 ν(O–H); 1546 ν(N=N). ^{1}H NMR (400 MHz, DMSO-d_6): δ 8.49 (s, 1H, OH), 7.77–6.67 (m, 9H, aromatic). ^{13}C NMR (100 MHz, DMSO-d_6): δ 161.15–106.30 (16C, aromatic).

H_2L^4. Yield: 66%. Anal. calcd for $C_{16}H_{11}BrN_2O_2$: C, 56.00; H, 3.23; N, 8.16. Found: C, 56.05; H, 3.22; N, 8.15. IR (KBr pellet, cm^{-1}): 3321 ν(O–H), 1587 ν(N=N). ^{1}H NMR (400 MHz, DMSO-d_6): δ 8.54 (s, 1H, OH), 7.75–6.45 (m, 9H, aromatic). ^{13}C NMR (100 MHz, DMSO-d_6): δ 149.77–114.98 (16C, aromatic).

Synthesis of oxidovanadium(IV) [$VO(L^{1-4})(L^{NN})$] compounds (1–5)

The complexes were prepared by refluxing an equimolar mixture of the metal precursor [$VO(acac)_2$], ligands(H_2L^{1-4}) and 2,2′-bipyridine (**1**, **3**, **4** and **5**) or 1,10-phenanthroline (**2**) in 20 mL of methanol under nitrogen atmosphere. After 3 h of reflux, brown colored crystals were obtained from the reaction mixture, which were filtered off, washed thoroughly with methanol, and dried. Some crystals were of diffraction quality and used directly for X-ray structure determination using a single crystal X-ray diffractometer.

$[V^{IV}O(L^1)(bipy)]\cdot H_2O$ (1). Yield: 60%. Anal. calcd for $C_{26}H_{20}N_4O_4V$: C, 62.03; H, 4.00; N, 11.31. Found: C, 62.07; H, 3.73; N, 11.53. IR (KBr pellet, cm^{-1}): 3582 ν(H_2O); 1506 ν(N=N); 955 ν(V=O). UV-vis (DMSO) [λ_{max}, nm (ε, M^{-1} cm^{-1})]: 800(92), 550(5203), 360(1483), 234(7833). ESI-MS: m/z 485 $[M - H_2O]^+$.

$[V^{IV}O(L^1)(phen)]$ (2). Yield: 60%. Anal. calcd for $C_{28}H_{18}N_4O_3V$: C, 66.02; H, 3.56; N, 11.00. Found C, 66.01; H, 3.53; N, 11.05. IR (KBr pellet, cm^{-1}): 1516 ν(N=N); 952 ν(V=O). UV-vis (DMSO) [λ_{max}, nm (ε, M^{-1} cm^{-1})]: 798(96), 532(5583), 362(1533), 267(9083). ESI-MS: m/z 509 $[M]^+$.

$[V^{IV}O(L^2)(bipy)]$ (3). Yield: 64%. Anal. calcd for $C_{27}H_{20}N_4O_3V$: C, 64.93; H, 4.04; N, 11.22. Found C, 64.96; H, 4.08; N, 11.20. IR (KBr pellet, cm^{-1}): 1508 ν(N=N); 959 ν(V=O). UV-vis (DMSO) [λ_{max}, nm (ε, M^{-1} cm^{-1})]: 789(90), 528(5000), 357(1493), 273(10 083). ESI-MS: m/z 499 $[M]^+$.

$[V^{IV}O(L^3)(bipy)]$ (4). Yield: 65%. Anal. calcd for $C_{26}H_{17}N_5O_5V$: C, 58.88; H, 3.23; N, 13.20. Found C, 58.90; H, 3.22; N, 13.21 IR (KBr pellet, cm^{-1}): 1516 ν(N=N); 959 ν(V=O). UV-vis (DMSO) [λ_{max}, nm (ε, M^{-1} cm^{-1})]: 792(94), 574(4917), 389(1333), 263(7167). ESI-MS: m/z 530 $[M]^+$.

$[V^{IV}O(L^4)(bipy)]$ (5). Yield: 68%. Anal. calcd for $C_{26}H_{17}BrN_4O_3V$: C, 55.34; H, 3.04; N, 9.93. Found: C, 55.34; H, 3.02; N, 9.92. IR (KBr pellet, cm^{-1}): 1552 ν(N=N); 965 ν(V=O). UV-vis (DMSO) [λ_{max}, nm (ε, M^{-1} cm^{-1})]: 794(93), 541(5333), 361(1483), 269(11 750). ESI-MS: m/z 564 $[M]^+$.

X-ray crystallography

Crystallographic data of the compounds **1** (color: black; size: 0.07 × 0.06 × 0.02 mm^3; prism), **2** (color: orange, size: 0.07 × 0.05 × 0.02 mm^3; shard), **3** (color: black; size: 0.15 × 0.14 × 0.13 mm^3; prism), **4** (color: black golden; size: 0.50 × 0.07 × 0.04 mm^3; needle) and **5** (color: black; size: 0.33 × 0.07 × 0.05 mm^3; prism) and details of refinement are summarized in Table 1.

Inclusion-free prismatic single crystals of all the five compounds were used to record the intensity data and cell parameters at 100(2) K on a Bruker APEX II single crystal X-ray diffractometer, Mo-radiation. The collected data were processed using SAINT and SADABS within the APEX2 software package by Bruker.[40] The structures were solved by direct methods (SHELXS, SIR97[41]) for compounds **1** and **2**, (SHELXT[42] or SIR97[41]) for compounds **3–5** and refined on F^2 by full-matrix least-squares procedures, using SHELXL.[43,44] The non-hydrogen atoms were refined anisotropically by full-matrix least-squares. Scattering factors are from Waasmair and Kirfel.[45] All hydrogen atoms were placed at calculated positions and refined using a riding model with C···H distances in the range 0.95–1.00 Å.

DFT calculations

DFT calculations were performed with the Gaussian 09 (revision D.01) software.[46] The geometries and harmonic frequencies of the complexes **1–5** were computed at the B3P86/6-311g level of theory as reported for other V complexes.[47] The calculation of the isotropic ^{51}V hyperfine coupling constants tensor **A** was performed on the optimized structures at the BHandHLYP/6-311+g(d) level of theory.[48] The theory background was described in the literature.[49]

DNA binding

The DNA binding experiments were performed in 50 mM Tris–HCl buffer (pH 8.0) with a Shimadzu spectrophotometer (UV-2450) using a fixed concentration of metal complex (25 μM) but variable CT-DNA concentrations ranging from 0 to 100 μM. Binding of ligands to CT-DNA was also studied. For this, a fixed concentration of ligand [25 μM in 50 mM Tris–HCl buffer (pH 8.0)] was titrated with variable DNA concentrations ranging from 0 to 100 μM.

Table 1 Crystal data and refinement details for complexes **1–5**

Complex	**1**	**2**	**3**	**4**	**5**
Empirical formula	$C_{26}H_{20}N_4O_4V$	$C_{28}H_{18}N_4O_3V$	$C_{27}H_{20}N_4O_3V$	$C_{26}H_{17}N_5O_5V$	$C_{26}H_{17}BrN_4O_3V$
Mass	503.40	509.40	499.41	530.39	564.28
Temperature	100(2) K	100(2) K	100(2) K	100(2) K	100(2) K
Wavelength	0.71073 Å	0.71073 Å	0.71073 Å	0.71073 Å	0.71073 Å
Crystal system	Triclinic	Triclinic	Monoclinic	Monoclinic	Monoclinic
Space group	$P\bar{1}$	$P\bar{1}$	$P2_1/c$	$P2_1/c$	$P2_1/c$
Unit cell dimensions	a = 8.6015(7) Å b = 10.3718(9) Å c = 12.5377(11) Å α = 93.200(6)° β = 90.428(5)° γ = 104.447(5)°	a = 8.148(2) Å b = 9.459(3) Å c = 14.752(4) Å α = 93.473(18)° β = 93.065(18)° γ = 109.172(15)°	a = 9.8888(9) Å b = 18.6789(15) Å c = 24.445(2) Å α = = 90° β = 98.725(5)° γ = 90°	a = 8.4764(7) Å b = 16.7531(13) Å c = 16.4889(14) Å α = 90° β = 103.846(4)° γ = 90°	a = 8.4333(5) Å b = 16.6359(10) Å c = 16.7706(11) Å α = 90° β = 103.479(3)° γ = 90°
Volume	1081.20(16) Å^3	1068.6(5) Å^3	4463.1(7) Å^3	2273.5(3) Å^3	2288.0(2) Å^3
Z	2	2	8	4	4
Density (calculated)	1.546 Mg m^{-3}	1.583 Mg m^{-3}	1.486 Mg m^{-3}	1.550 Mg m^{-3}	1.638 Mg m^{-3}
Absorption coefficient	0.503 mm^{-1}	0.507 mm^{-1}	0.484 mm^{-1}	0.487 mm^{-1}	2.218 mm^{-1}
F(000)	518	522	2056	1084	1132
Θ range for data collection	1.627–28.313°	1.387–25.401°	1.378–28.432°	1.759–28.497°	1.749–28.442°
Reflections collected	9623	6036	21 870	11 204	11 239
Independent reflections	5105 [R(int) = 0.0443]	3909 [R(int) = 0.0675]	11 119 [R(int) = 0.0354]	5716 [R(int) = 0.0297]	5732 [R(int) = 0.0224]
Completeness to Θ = 25.00°	96.7%	99.6%	99.9%	100.0%	100.0%
Limiting indices	$-11 \le h \le 11$, $-13 \le k \le 13$, $-16 \le l \le 16$	$-9 \le h \le 9$, $-11 \le k \le 9$, $-17 \le l \le 17$	$-13 \le h \le 13$, $-24 \le k \le 24$, $-32 \le l \le 32$	$-11 \le h \le 11$, $-22 \le k \le 22$, $-21 \le l \le 22$	$-11 \le h \le 11$, $-22 \le k \le 22$, $-22 \le l \le 22$
Refinement method	Full-matrix least-squares on F^2	Full-matrix least-squares on F^2	Full-matrix least-squares on F^2	Full-matrix least-squares on F^2	Full-matrix least-squares on F^2
Data/restraints/parameters	5105/6/337	3909/36/325	11 119/0/633	5716/0/334	5732/0/316
Goodness-of-fit on F^2	1.037	1.002	1.032	1.007	1.028
Final R indices [$I > 2\sigma(I)$]	R_1 = 0.0463, wR_2 = 0.0934	R_1 = 0.0631, wR_2 = 0.1220	R_1 = 0.0422, wR_2 = 0.0946	R_1 = 0.0357, wR_2 = 0.0827	R_1 = 0.0262, wR_2 = 0.0610
R indices [all data]	R_1 = 0.0802, wR_2 = 0.1058	R_1 = 0.1282, wR_2 = 0.1464	R_1 = 0.0707, wR_2 = 0.1096	R_1 = 0.0649, wR_2 = 0.0953	R_1 = 0.0377, wR_2 = 0.0651
Largest diff. peak and hole	0.722 and −0.448 e Å^{-3}	0.610 and −0.491 e Å^{-3}	0.382 and −0.517 e Å^{-3}	0.268 and −0.450 e Å^{-3}	0.565 and −0.392 e Å^{-3}
CCDC deposition number	1907845	1907846	1907847	1907848	1907844

Competitive DNA binding by fluorescence measurements

Three fluorescent dyes namely 4′,6-diamidino-2-phenylindole (DAPI), methyl green (MG) and ethidium bromide (EB) were used to study competitive binding of the complexes **1–5** with CT-DNA by using a Fluoromax 4P spectrofluorometer (Horiba Jobin Mayer, USA). On increasing the concentration of the complex, EB binds to the CT-DNA by intercalation whereas DAPI and MG bind to the minor and major grooves of the DNA, respectively.[7c]

BSA binding

Fluorescence quenching experiments were carried out to examine the interaction between BSA and the mixed ligand oxidovanadium(IV) complex in 50 mM Tris–HCl buffer (pH 8). In this method, 10 μM of BSA along with the increased concentrations (0–100 μM) of the complex was excited at 295 nm and the emission intensities of BSA were recorded at 340 nm for the calculation of quenching parameters.

Cytotoxicity studies

MTT assay. A549 (lung cancer) cells cultured in RPMI 1640 containing 10% FBS and penicillin (100 U mL^{-1}) in a humidified 5% CO_2 incubator at 37 °C were used. The cytotoxicity was assayed by determining the viability of A549 cells after treatment by **1–5** by MTT assay. The cells were seeded in 96 well plates at a concentration of 10^5 cells per well. After confluency, treatment was given with varying concentrations (5, 15, 25, 50 and 100 μM) of the complexes. The complexes were dissolved in DMSO at a concentration of 500 μM and then suitably diluted in plain DMEM. Final working concentration of DMSO was kept less than 2%. IC_{50} was calculated for each compound by treating the cells for 48 h.

Propidium iodide staining. Treated and untreated A549 cells with different concentrations 5, 15, 25, 50 and 100 μM of the complexes were incubated for 48 hours, after that fixed with 3.7% of formaldehyde for 15 min and washed twice with PBS, followed by treatment with 0.2% Triton-X 100 in PBS for 30 seconds and washing with PBS. Finally propidium iodide solution (10 μg mL^{-1}) was added and kept for 15 min in the dark, and then the cells were washed twice with PBS and imaged under a fluorescence microscope (Olympus IX 70).

Results and discussion

Synthesis

Five mixed ligand oxidovanadium(IV) complexes were synthesized by refluxing an equimolar ratio of $[VO(acac)_2]$, a tridentate arylazo ligand (H_2L^{1-4}) and a bidentate polypyridyl ligand bpy (**1**, **3**, **4** and **5**) and phen (**2**) in methanol under inert atmosphere which is summarized in Scheme 1. The detailed methods used for the syntheses of oxidovanadium(IV) are given in the Experimental section. The solution state stability of **1–5** was further analysed in Tris–HCl buffer over a period of 72 h by time-dependent UV/vis (Fig. S1, ESI†) spectroscopy.

Spectral characteristics

The IR spectra of the ligands, H_2L^{1-4}, and synthesized metal complexes (**1–5**) are given in the Experimental section. A band in the region of 3321–3448 cm^{-1} in the ligands is assigned to the stretching vibration of aromatic O–H in the phenolic moiety.[7b,c,e,f,g,37b,c,50] The VO(IV) mononuclear mixed ligand complex does not show the band in a range of 3321–3448 cm^{-1}, indicating the OH hydrogen is deprotonated after complexation. However in complex **1** a new band found at 3582 cm^{-1} may be assigned to H_2O molecules in the crystal structure of $[VO(L^1)bipy]\cdot H_2O$. The IR spectra of all the complexes show a single N=N stretch in the range of 1506 to 1552 cm^{-1}, which is considerably lower than that of the free ligand in the range of 1545 to 1587 cm^{-1} which might be attributable to the coordination to the metal atom. Furthermore, the ν(V=O) stretch of the

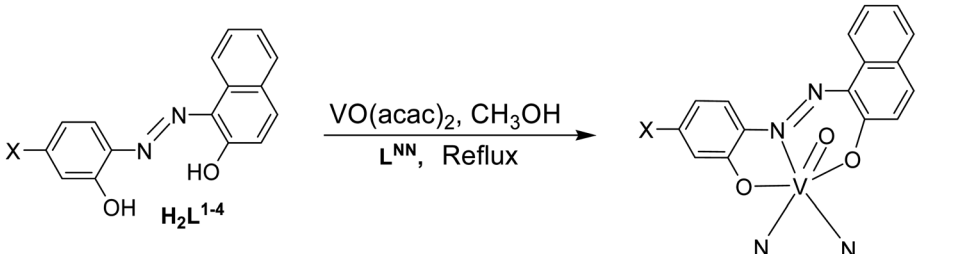

Ligand	X	L^{NN}	Complex
H_2L^1	H	bipy	$[V^{IV}O(L^1(bipy)].(H_2O)$ (1)
H_2L^1	H	phen	$[V^{IV}O(L^1)(phen)]$ (2)
H_2L^2	CH_3	bipy	$[V^{IV}O(L^2)(bipy)]$ (3)
H_2L^3	NO_2	bipy	$[V^{IV}O(L^3)(bipy)]$ (4)
H_2L^4	Br	bipy	$[V^{IV}O(L^4)(bipy)]$ (5)

$[V^{IV}OL^{1-4}(L^{NN})]$(1- 5)

Scheme 1 Schematic representation for the synthesis of $[V^{IV}O(L^{1-4})(L^{NN})]$ (**1–5**).

complexes occurs in the 950–970 cm^{-1} range which is in the usual range (960 ± 50 cm^{-1}) observed for the majority of oxidovanadium(IV) complexes.[7b,c,e,f,g,37b,c,51]

Electronic absorption spectra of complexes **1–5** were recorded in DMSO which are given in the Experimental section. All of the complexes exhibit three intensity bands in the range 580–234 nm, among which the two absorption bands in the UV region (389–234 nm) are attributed to the ligand centered transitions, whereas the lowest energy absorption is observed in the visible range, λ_{max} = 574–528 nm due to the LMCT transition.[7g,52] The low intensity band in the range of 800–790 nm is due to d–d transition.[7f]

^1H and ^{13}C NMR of the ligands (H_2L^{1-4}) were recorded in DMSO-d_6. The ^1H NMR spectra of the free ligands exhibit signals in the range δ 9.73–8.49 ppm which are attributable to the phenolic –OH proton of the arylazo ligand. The aromatic protons of each of the ligands have resonated as multiplets in the region, δ 8.50–6.45 ppm. The peaks observed in the ^{13}C NMR spectra in the region of δ 161.15–106.30 ppm are assigned to aromatic carbons, while the aliphatic protons ($-CH_3$) for ligand H_2L^2 appear at δ 21.66 ppm.[7g]

EPR spectroscopy

EPR spectra were recorded on the bipy derivatives **1**, **3–5** in the solid state and after dissolution in DCM. The spectra recorded on the solid compounds were characterized by an isotropic absorption centred at a g factor in the range 1.974–1.987 (Table 2). A g value lower than 2 is expected for a $V^{IV}O$ ion with a d^1 electronic configuration.[53] The broad signal is typical for solid samples and is due to a mixture of intercenter exchange and dipolar interactions.[54] The experimental and simulated spectra of **5** are reported as an example in Fig. S2 (ESI†).

When the spectra were recorded on the complexes dissolved in an organic solution (DCM), isotropic signals were obtained with eight lines due to the coupling between the unpaired electron and nucleus of ^{51}V (I = 7/2, 99.8% natural abundance). Only one set of resonances is revealed indicating that **1–5** maintain in solution their hexa-coordinated structure (see Fig. 1 showing the spectrum of complex **5**). The values of g_{iso} are 1.965–1.966 and $|A_{iso}|$ 100.8–101.8 × 10^{-4} cm^{-1} (Table 2). The ^{51}V isotropic hyperfine coupling constants were calculated by DFT methods using the BHandHLYP functional which, as substantiated in the literature,[49] slightly underestimates A_{iso} and the values found are in agreement with what was expected (percent deviations with respect to the experimental values between −4.4 and −5.5%).

Table 2 Experimental and calculated spin Hamiltonian parameters for the $V^{IV}O$ complexes with bipy as the co-ligand **1**, **3–5**

	Solid state	Solution		Calculated
Complex	g_{iso}	g_{iso}	$A_{iso}/10^{-4}$ cm^{-1}	$A_{iso}/10^{-4}$ cm^{-1} [a]
1	1.974	1.965	−100.8	−95.9
3	1.979	1.966	−101.8	−96.2
4	1.987	1.965	−101.0	−96.6
5	1.977	1.965	−101.2	−96.1

[a] Calculated at the BHandHLYP/6-311+g(d) level of theory.

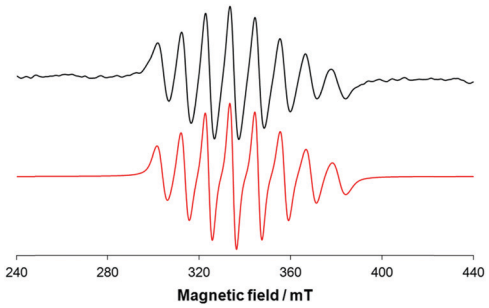

Fig. 1 Experimental (in black) and simulated with the software WINEPR SimFonia (in red) isotropic EPR spectra of complex **5**.

Electrochemical properties

The electrochemical properties of all the complexes (**1–5**) have been examined by cyclic voltammetry at 100 mV s^{-1} scan rate in acetonitrile solution in the presence of 0.1 M TBAP as an electrolyte using a Pt as a working as well as an auxiliary electrode and SCE as a reference electrode. The cyclic voltammograms of **1–5** show a similar type of pattern (Fig. 2 represents the cyclic voltammogram of complex **1** and rest of the cyclic voltammograms of complexes **2–5** are depicted in Fig. S3, ESI†) and their redox potential data have been summarized in Table 3. From the voltammograms it is observed that in the cathodic region all the complexes exhibit a quasi-reversible single-electron wave at an $E^c_{1/2}$ value in the range of −1.29 to −1.37 V due to the reduction

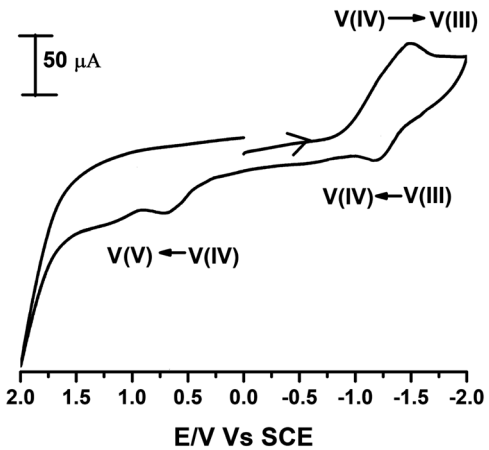

Fig. 2 Cyclic voltammogram of $[V^{IV}OL^1(bipy)]\cdot H_2O$ (**1**).

Table 3 Cyclic voltammetric results of complexes **1–5** at 298 K in acetonitrile[a]

Complex	E_{Pa} (V)	$E^c_{1/2}$ (V)	ΔE_P (mV)
1	0.66	−1.34	260
2	0.37	−1.29	220
3	0.64	−1.32	256
4	0.67	−1.37	262
5	0.62	−1.30	255

[a] In acetonitrile at a scan rate of 100 mV s^{-1}. $E^c_{1/2} = (E_{Pa} + E_{Pc})/2$, where E_{Pa} and E_{Pc} are anodic and cathodic peak potentials *vs.* SCE, respectively. $\Delta E_P = E_{Pa} - E_{Pc}$.

of the V(IV) center to V(III).[7f] In the anodic region an irreversible single electron response observed due to the V(IV)/V(V) oxidation was observed for the complexes containing bipy as co-ligand (**1**, **3**, **4** and **5**) at the potential window of 0.62 to 0.67 V, and at 0.37 V for complex **2** containing phen as co-ligand.[55] The corresponding single electron oxidation and reduction peaks observed in the CVs of each complex (**1**–**5**) were confirmed by comparing the voltammograms at different scan rates maintaining the identical experimental conditions and by comparing the current height with that of the standard ferrocene/ferrocenium couple.

Description and DFT prediction of X-ray structures

The molecular structures of complexes (**1**–**5**) are shown in Fig. 3 and some important bond distances and angles are collected in Table 4. Single crystal X-ray structural analysis shows that

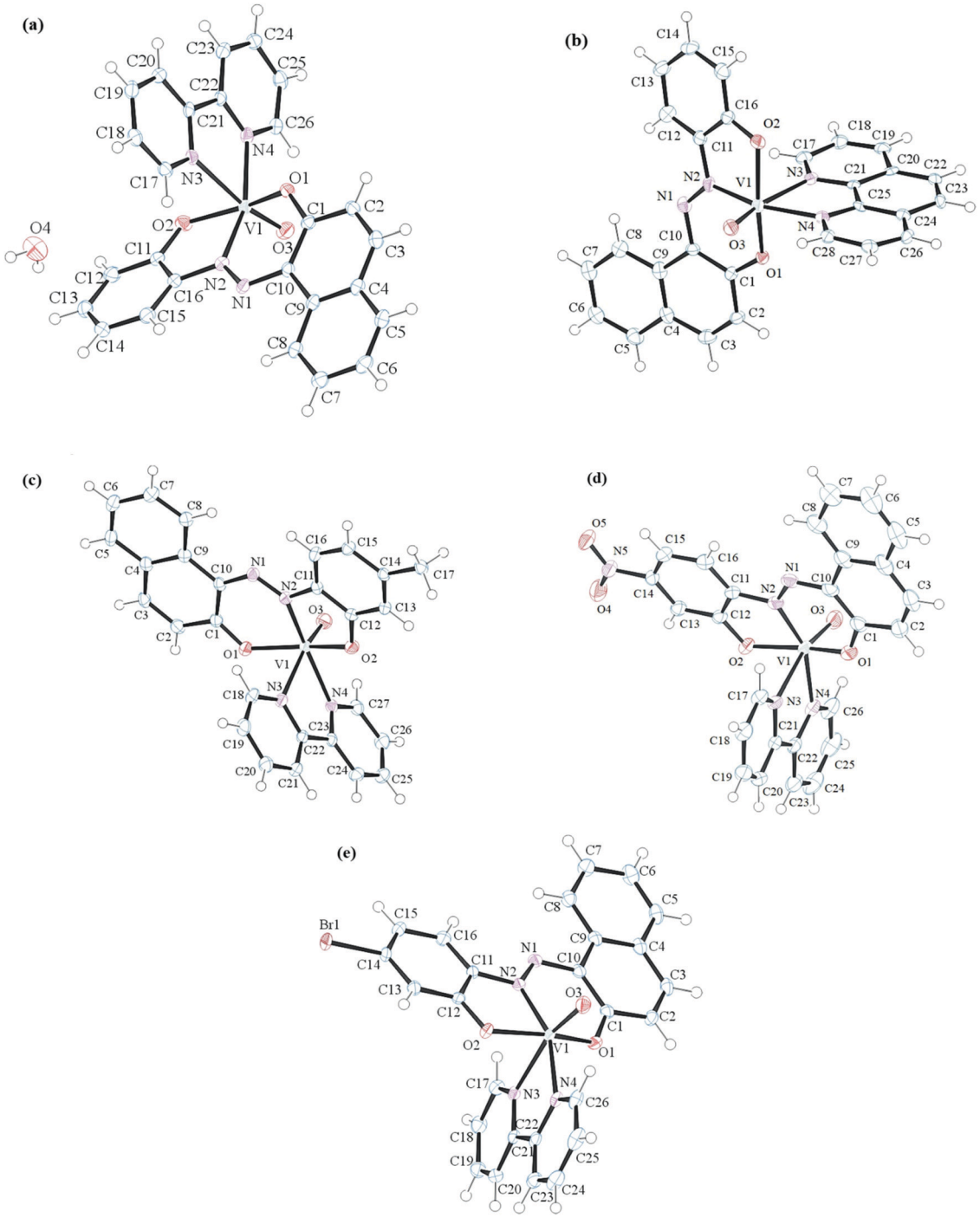

Fig. 3 ORTEP diagrams of compounds (a) $[V^{IV}OL^{1}(bipy)]\cdot H_2O$ (**1**), (b) $[V^{IV}OL^{1}(phen)]$ (**2**), (c) $[V^{IV}OL^{2}(bipy)]$ (**3**), (d) $[V^{IV}OL^{3}(bipy)]$ (**4**) and (e) $[V^{IV}OL^{4}(bipy)]$ (**5**) with thermal ellipsoids at the 50% probability level.

Table 4 Selected bond lengths [Å] and angles (°) for complexes **1–5**

Complexes	1	2	3	4	5
Bond lengths [Å]					
V(1)–O(1)	1.9692(15)	1.967(3)	1.9735(15)	1.9851(13)	1.9808(12)
V(1)–O(2)	1.9721(15)	1.969(3)	1.9632(15)	1.9696(13)	1.9713(12)
V(1)–O(3)	1.6059(16)	1.607(3)	1.6075(15)	1.6036(13)	1.6063(13)
V(1)–N(2)	2.056(2)	2.063(4)	2.0711(18)	2.0533(15)	2.0642(15)
V(1)–N(3)	2.3308(19)	2.357(3)	2.3380(18)	2.3080(14)	2.3134(14)
V(1)–N(4)	2.132(2)	2.136(4)	2.1669(17)	2.1277(15)	2.1365(15)
N(1)–N(2)	1.294(3)	1.286(5)	1.284(2)	1.294(2)	1.2901(19)
Bond angles (°)					
O(1)–V(1)–O(2)	157.12(7)	155.42(12)	154.65(7)	157.30(6)	156.22(5)
O(1)–V(1)–O(3)	99.34(8)	100.85(14)	98.79(7)	96.95(7)	97.48(6)
O(2)–V(1)–O(3)	101.25(8)	102.06(14)	104.14(7)	103.53(6)	104.18(6)
O(1)–V(1)–N(2)	83.92(7)	84.43(14)	84.53(7)	84.79(6)	84.66(5)
O(2)–V(1)–N(2)	81.20(7)	81.32(15)	80.34(7)	80.48(5)	80.71(5)
O(3)–V(1)–N(2)	105.06(8)	104.63(14)	101.89(7)	105.31(7)	104.10(6)
O(1)–V(1)–N(3)	79.75(6)	79.43(12)	80.41(6)	78.38(5)	77.72(5)
O(2)–V(1)–N(3)	82.11(6)	80.01(12)	80.65(6)	83.99(5)	83.53(5)
O(3)–V(1)–N(3)	168.18(8)	167.96(14)	163.39(7)	165.25(6)	165.05(6)
N(3)–V(1)–N(4)	72.83(7)	73.25(13)	71.12(6)	72.34(5)	72.24(5)
O(1)–V(1)–N(4)	95.99(7)	93.22(13)	104.85(6)	102.68(5)	102.78(5)
O(2)–V(1)–N(4)	91.84(7)	93.61(14)	84.66(6)	85.21(5)	84.99(5)
O(3)–V(1)–N(4)	95.63(8)	94.75(14)	93.28(7)	95.40(7)	95.40(6)
N(2)–V(1)–N(3)	86.62(7)	87.39(13)	94.57(6)	88.31(5)	89.66(5)
N(2)–V(1)–N(4)	159.07(7)	160.58(13)	160.83(7)	157.05(6)	158.10(6)

complexes **1** and **2** crystallize in triclinic space group $P\bar{1}$ while complexes **3**, **4**, and **5** are monoclinic with space group $P2_1/c$. In all the five complexes the monomeric hexacoordinated V(IV) centers are distorted octahedrally coordinated. The tridentate arylazo ligand (H_2L^{1-4}) places equatorially to a VO^{2+} moiety, leaving the ancillary ligand, namely 2,2′-bipyridine and 1,10-phenanthroline, to bind axial-equatorially. In the case of complex **1**, one disordered water molecule is present. The V═O distances for all the five complexes lie within the range of 1.605–1.607 Å which is comparable to the reported lengths from 1.59 to 1.62 Å for most other VO^{2+} complexes.[7g,56] The unequal lengths of the V(1)–O(1), V(1)–O(2), V(1)–O(3), V(1)–N(2), V(1)–N(3) and V(1)–N(4) bonds and differing angles generated by these bonds cause the distortion of the vanadium coordination octahedron. Specifically, the crystallographic data reveal that the length of the V–N(azo) bond is shorter than that of V–$N_{bipy/phen}$ which is indicative of a stronger binding affinity of the arylazo ligand towards the vanadium center than that of bipy/phen. The stronger *trans* effect of the terminal V═O bond causes the V^{IV}–$N_{bpy/phen}$ bond *trans* to the V═O bond to be longer than the other V^{IV}–$N_{bpy/phen}$ bond.[7g]

The structure of **1–5** was also optimized by DFT methods according to the procedure established in the literature.[47] Based on the experimental XRD analysis, for all the species a distorted octahedral geometry was considered with the tridentate ligand on the equatorial plane in a *mer* fashion and the co-ligand in an equatorial-axial arrangement. In Table S1 of the ESI† the comparison between selected experimental and calculated bond lengths and angles for **1–5** is summarized, while in Fig. S4 (ESI†) the overlap of the XRD and DFT optimized structures is shown. The agreement is very good with a mean absolute percent deviation of 0.5% for the bond lengths, and 2.6% for the bond angles, the maximum percent deviation being between −1.2 and 0.9% for the distances and between −5.6 and 5.0% for the angles. These optimized structures were used to calculate the ^{51}V **A** tensor (see above).

DNA binding

Binding of the mixed ligand oxidovanadium(IV) complexes (**1–5**) with CT-DNA was studied *via* the absorption spectroscopic method. As a representative the electronic spectra of the complex **2** in the absence and presence of CT-DNA is shown in Fig. 4 whereas the rest of the spectra are depicted in Fig. S5 (ESI†). For this experiment 25 μM of metal complexes were titrated with increasing amounts of CT-DNA in the range from

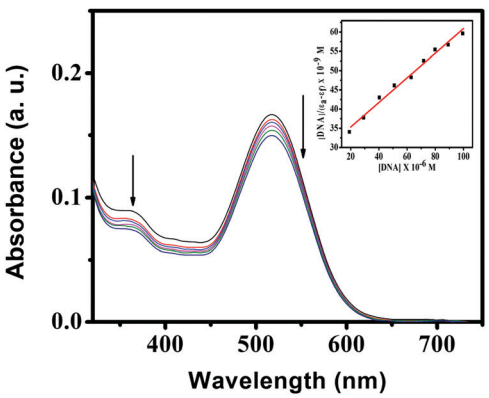

Fig. 4 Absorption spectroscopic study of complex **2** (25 μM) with increasing concentrations of CT-DNA (0–100 μM) in 50 mM Tris–HCl buffer (pH 8.0). The arrow shows the changes in absorbance with respect to an increase in the CT-DNA concentration. The inset shows the linear fit of [DNA]/($\varepsilon_a - \varepsilon_f$) *vs.* [DNA].

0 to 100 μM. The complexes show absorption bands in the region 580–357 nm. The lower energy absorption in the visible range, λ_{max} = 574–528 nm and the bands in the higher energy UV absorption region, 389–357 nm are attributed to a L–V(dπ) ligand to metal charge transfer (LMCT) and intraligand transitions, respectively. With increasing concentration of CT-DNA, the complexes showed a hypochromic shift in both the LMCT and intra-ligand transition bands. This hypochromicity is due to strong stacking interaction between the aromatic chromophore of the ligand and DNA base pairs.[7b–e,57,58] To determine the binding affinity of the complexes with CT-DNA, the binding constant, K_b was calculated through the following equation:

$$\frac{[DNA]}{\varepsilon_a - \varepsilon_f} = \frac{[DNA]}{\varepsilon_b - \varepsilon_f} + \frac{1}{K_b(\varepsilon_b - \varepsilon_f)} \quad (1)$$

where [DNA] is the concentration of DNA base pairs, and ε_a, ε_f and ε_b correspond to apparent extinction coefficients for the complex *i.e.* Abs/[complex] in the presence of DNA, in the absence of DNA and to fully bound DNA, respectively. A plot of $[DNA]/(\varepsilon_a - \varepsilon_f)$ *vs.* [DNA] gave a slope and the intercept equal to $1/(\varepsilon_b - \varepsilon_f)$ and $1/K_b(\varepsilon_b - \varepsilon_f)$, respectively, while the binding constant K_b was calculated from the ratio of the slope to the intercept. The binding constant of the complexes followed an order of **2** > **4** > **1** > **3** > **5** and has been given in Table 5. The order of the binding affinity can be described on the basis of the presence of a different co-ligand in the complexes and incorporation of the electron withdrawing and electron releasing groups attached to the aromatic rings in the ligands.[59,60] Among all, complex **2** shows the highest binding affinity compared to the other complexes which may be due to the presence of phen as co-ligand.[59] Comparing the binding affinity of the other four complexes, the maximum binding affinity of complex **4** and the lowest values of complexes **3** and **5** may be due to the presence of electron withdrawing (NO_2 and Br) and releasing (CH_3) groups, respectively,[60] whereas complex **1** shows a value in between because it has neither an electron-withdrawing nor a releasing group in the ligand. We had also studied the binding affinity of the ligands; however, it was found to be significantly lower than that of the complexes (Fig. S6 and Table S2, ESI†).

Table 5 DNA binding parameters for **1–5**

Complexes	Binding constant $(K_b)^a$ (M^{-1})
1	1.60×10^4
2	2.03×10^4
3	1.50×10^4
4	1.70×10^4
5	7.10×10^3

[a] DNA binding constants were determined by the UV-vis spectral method.

Competitive binding studies

The investigation of the binding mode of the present complexes with CT-DNA was carried out through competitive binding experiments by fluorescence spectroscopy.[61] These experiments are generally performed with three fluorescent dyes, namely 4,6-diamidino-2-phenylindole (DAPI), methyl green (MG) and ethidium bromide (EB). EB binds to DNA though the intercalation mode, whereas DAPI and MG bind through the minor groove and major groove of the DNA, respectively.[7c,e]

Ethidium bromide (EB) displacement experiment. The binding of complexes to CT-DNA was studied by considering the quenching of the fluorescence emission from EB bound CT-DNA on successive addition of the complexes. On increasing the concentration of complex the emission intensity of EB is decreased due to the displacement of EB from CT-DNA. This clearly indicates that EB molecules are displaced from their CT-DNA binding sites by the complexes.[62,63] The efficiency of fluorescence quenching can be calculated by using the Stern–Volmer equation. The K_q values for complexes (**1–5**) lie in the range 3.4×10^{13}–7.6×10^{12} M^{-1} s^{-1} which were obtained from the slope of a linear plot of F_0/F *versus* [Q]. Among all, complex **4** showed the highest quenching of EB bound to CT-DNA fluorescence intensity at 600 nm *i.e.* 95%. The fluorescence quenching curves of EB bound to CT-DNA in the presence of the complexes and the Stern–Volmer plots of fluorescence titrations of the complexes with CT-DNA are shown in Fig. 5 and Fig. S7 (ESI†). These studies suggest that the complexes (**1–5**) can bind to CT-DNA *via* an intercalative mode.

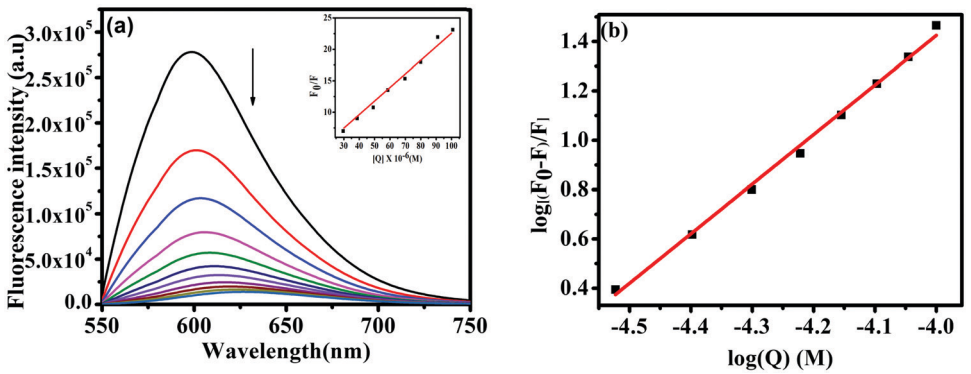

Fig. 5 (a) Fluorescence quenching of EB (10 μM) by complex $[V^{IV}O(L^3)(bipy)]$ (**4**) (0–100 μM) and the inset shows the Stern–Volmer plot of complex $[V^{IV}O(L^3)(bipy)]$ (**4**); (b) the Scatchard plot of complex $[V^{IV}O(L^3)(bipy)]$ (**4**).

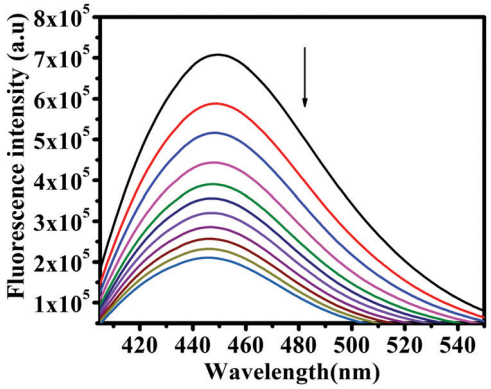

Fig. 6 Fluorescence quenching of DAPI (10 μM) by complex $[V^{IV}O(L^1)(bipy)]\cdot H_2O$ (**1**) (0–100 μM).

4′,6-Diamidino-2-phenylindole (DAPI) displacement experiment. To confirm the minor groove competitive binding, experiments were carried out by titrating DAPI bound CT-DNA solution with increasing amounts of complexes. On successive addition of the complexes to DAPI bound CT-DNA, the emission intensity decreases at 449 nm which is due possibly to the displacement of the DAPI bound to CT-DNA by the complexes.[7e] The K_q values for complexes (**1–5**) lie in the range 3.5×10^{12}–3.3×10^{12} M^{-1} s^{-1} which were obtained from the slope of a linear plot of F_0/F *versus* [Q]. Among all the complexes, **1**, **2** and **5** show the highest quenching, 70%, of DAPI bound to CT-DNA having fluorescence intensity at 449 nm (Fig. 6 and Fig. S8, ESI†). Therefore, it can be deduced that these complexes can also bind to the CT-DNA *via* a minor groove binding mode.

Methyl green (MG) displacement experiment. Similar experiments were performed with MG bound CT-DNA with increasing concentrations of **1–5**. Upon the addition of the complexes to MG bound CT-DNA we did not observe any significant change in fluorescence intensity of MG. This implies that these complexes do not interact with CT-DNA *via* a major groove binding mode.

Hence, from the above experiments it can be concluded that these complexes (**1–5**) interact with CT-DNA *via* both intercalative and minor groove binding modes.[7e,62,63]

Protein binding

The protein binding studies with **1–5** were also performed *via* tryptophan emission quenching experiments.[7d] Three amino acids such as tryptophan, tyrosine, and phenylalanine are generally responsible for showing fluorescence intensity of BSA protein[64] showing emission at 347 nm due to the presence of tryptophan residues in its amino acid sequence. To predict the quenching of these residues by the complexes we have studied their interactions with BSA in the wavelength range of 305–500 nm upon excitation at 295 nm. For this purpose 10 μM of BSA was titrated with different concentrations of complexes (0–100 μM) and it is observed that the fluorescence intensity gradually decreases (Fig. S9, ESI†). Upon successive addition of the complexes, the fluorescence intensity at 347 nm is decreased due to the interactions of the complexes with the BSA protein along with blue shift in complexes **1**, **3**, **4** and **5**, and red shift in complex **2**. Among the complexes, **4** shows the highest binding affinity towards BSA. All the spectra are given in Fig. 7 and Fig. S10 (ESI†). This quenching effect may be due to the changes in the secondary structure of BSA.[65] The quenching effect was further determined by the Stern–Volmer equation (Table 6).

$$\frac{F_0}{F} = 1 + K_q\tau_0[Q] = 1 + K_{SV}[Q] \quad (2)$$

where F_0 and F are the fluorescence intensities of BSA solution in the absence and presence of a quencher, respectively, [Q] is the concentration of a quencher, τ_0 is the average bimolecular lifetime in the absence of the quencher and K_q is the bimolecular quenching rate constant, and K_{SV} is the Stern–Volmer quenching constant in M^{-1}. From the Scatchard equation we can calculate the binding constant (K_a) and the number of binding sites (n) which is given below (Table 6).

$$\log\frac{F_0 - F}{F} = \log K_a + n\log[Q] \quad (3)$$

The quenching constants (K_{SV}) for all the vanadium complexes lying in the range of 7.6×10^5–2.3×10^5 M^{-1} are given in Table 6 which revealed that the quenching ability of the complexes is in the order **4** > **1** > **3** > **5** > **2**. Similarly the binding constant (K_a) values and biomolecular rate constant (K_q) values

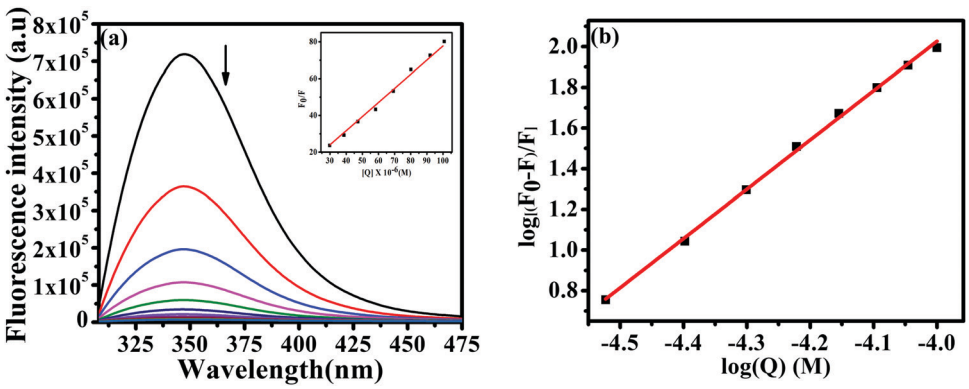

Fig. 7 (a) Fluorescence quenching of BSA (10 μM) by complex $[V^{IV}O(L^3)(bipy)]$ (**4**) (0–100 μM) and the inset shows the Stern–Volmer plot of complex $[V^{IV}O(L^3)(bipy)]$ (**4**); (b) the Scatchard plot of complex $[V^{IV}O(L^3)(bipy)]$ (**4**).

Table 6 BSA binding parameters of the complexes **1–5**

Complex	Stern–Volmer constant K_{SV} (M^{-1})	Bimolecular rate constant K_q (M^{-1} s^{-1})	Binding constant K_a (M^{-1})	Number of binding sites (n)
1	6.6×10^5	1.1×10^{14}	2.5×10^{11}	2.35
2	2.3×10^5	3.7×10^{13}	9.3×10^7	1.63
3	5.4×10^5	8.7×10^{13}	1.4×10^{10}	2.07
4	7.6×10^5	1.2×10^{14}	5.2×10^{11}	2.42
5	4.3×10^5	6.9×10^{13}	8.1×10^9	2.04

Table 7 IC_{50} value of the complexes **1–5**

Complexes	IC_{50} (μM) A549
1	49.66 ± 0.11
2	44.72 ± 0.04
3	53.80 ± 0.07
4	48.92 ± 0.30
5	57.54 ± 0.28
Pyriplatin	52.10 ± 2.30

of complexes followed the same order as observed for the quenching constant (K_{SV}) values towards BSA. We had also studied the binding affinity of the ligands, however it was found to be significantly lower than that of the complexes (Fig. S11 and Table S3, ESI†).

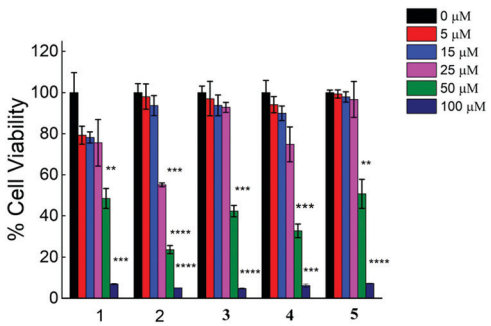

Fig. 8 Effect of the complexes (**1–5**) on cell viability of A549 cells. The cells were treated with different concentrations of the test compounds for 48 h and then cell viability was calculated by MTT assay. Data are presented as mean values ± SEM. Differences are considered statistically significant when $^{**}p \leq 0.01$, $^{***}p \leq 0.001$ and $^{****}p \leq 0.0001$.

Cytotoxicity

MTT assay. The anticancer activity of **1–5** has been studied against the A549 cell line *via* the MTT assay method.[66,67] The ligands, H_2L^{1-4} and $VO(acac)_2$ gave high IC_{50} values of >200 μM, whereas **1–5** gave values in the range 57.54–44.72 μM (Table 7 and Fig. 8). Standard drug pyriplatin (*cis*-diammine-(pyridine)chloroplatinum(II)) gives an IC_{50} value of 52.1 ± 2.3.[68] From the results, it was found that there is a significant increase in the antiproliferative efficacy of the metal complexes in comparison to their corresponding ligands, which indicates that the coordination of vanadium metal has a marked effect on their cytotoxicity. Among all the complexes, **2** showed the highest cytotoxicity, which may be due to the presence of phen as co-ligand,[59] while the other complexes showed cytotoxicity in the order of **2** > **4** > **1** > **3** > **5**. These results are in accord with the DNA binding ability of the complexes. Also, the variation of cytotoxicity of the complexes may be attributed to the presence of electron withdrawing (NO_2 and Br) and releasing (CH_3) groups, respectively.[7a] However, **1** shows a value in between, because of having neither an electron-withdrawing nor a releasing group in the ligand.[7a] These results show that the synthesized metal complexes exhibit greater cytotoxic activity than the free ligands which is agreement with previous reports.[7a–d,f,g]

MTT assay was also performed to determine the cytotoxicity of **1–5** on the HaCaT (immortalized human keratinocytes) cell line. The complexes gave high IC_{50} values (144.00–614.00 μM, Table S4, ESI†) and their cell viability (Fig. S12, ESI†) in HaCaT cells indicated that the compounds did not manifest any notable cytotoxicity to normal keratinocytes. It will be significant to mention here that we had also evaluated the cytotoxicity of the complexes against HeLa (cervical cancer) and HT-29 (colon cancer) cell lines; however, they gave high IC_{50} values of >100 μM. So it can be also be deduced that the complexes

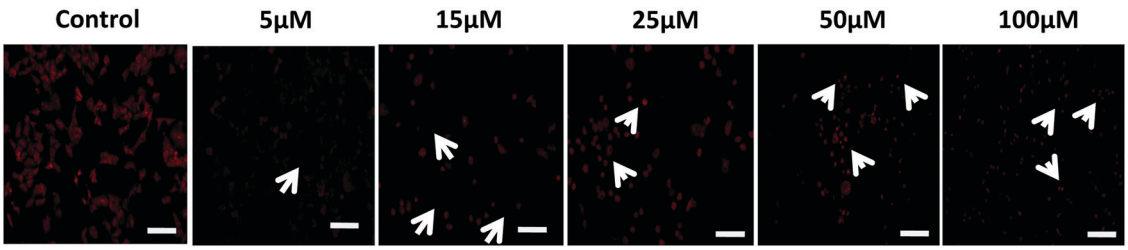

Fig. 9 PI staining of complex **2** of A549 (lung cancer line) taken using an Olympus IX 74 fluorescence microscope. Arrows showing the morphological changes in nuclei of A549 cells observed on applying increasing concentrations (5, 15, 25, 50 and 100 μM) of complex **2** at different concentrations in comparison to control. The scale bar corresponds to 100 μm.

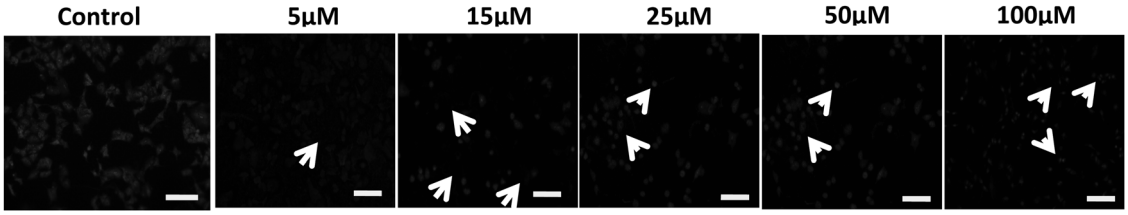

Fig. 10 Gray scale images of complex **2** of A549 (lung cancer line) taken using an Olympus IX 74 fluorescence microscope. Arrows showing the morphological changes in nuclei of A549 cells observed on applying increasing concentrations (5, 15, 25, 50 and 100 μM) of complex **2** at different concentrations in comparison to control. The scale bar corresponds to 100 μm.

are specific in cytotoxicity towards a particular cell line. This type of specificity has also been reported by ourselves earlier.[7g,69]

Propidium iodide staining. To study the effect of the treatment of the test complexes on live cells, propidium iodide staining was used.[69,70] Fig. 9 and Fig. S13 (ESI†) show images taken after PI staining in red fluorescence and the observed morphological changes in nuclei of A549 cells on applying increasing concentrations (5, 15, 25, 50 and 100 μM) of the complexes. Fig. 10 and Fig. S14 (ESI†) show the gray scale images after the treatment with increasing concentrations of **1–5**. It is observed that in comparison to the control, the treated wells show a reduced number of PI stained nuclei. This indicates that the complexes induce a dose dependent cell death in the cancer cells.[69] The arrows show nuclear condensation and fragmentation taking place in the treated cells. This type of dose dependent cell death in the cancer cells is well reported in the literature.[7f]

Conclusions

In summary, the synthesis of mixed ligand oxidovanadium(IV) complexes $[V^{IV}O(L^{1-4})(L^{NN})]$ (**1–5**) with tridentate binegative arylazo ligands containing an ONO donor atom and bidentate ancillary ligands (2,2′-bipyridine and 1,10-phenanthroline) is presented. All the complexes have been characterized by different spectroscopic methods, and molecular structures are provided by single crystal X-ray diffraction. X-ray crystallography reveals that hexacoordinated vanadium anions are located in a distorted octahedral geometry within the N_3O_3 donor environment where the tridentate arylazo ligand (H_2L^{1-4}) coordinates equatorially to a VO^{2+} moiety leaving the ancillary ligand to bind at the axial–equatorial positions. Further, the DNA binding activity of all the complexes has been investigated. The experimental results show that the complexes moderately bind with CT-DNA *via* both intercalative and minor groove modes with binding constants within the range of 7.1×10^3–2.03×10^4 M^{-1}. However compound **2** shows the highest binding affinity towards CT-DNA compared to the other complexes. The interaction of **1–5** with bovine serum albumin was also studied *via* tryptophan emission quenching experiments in order to understand the interaction of the complexes with serum albumins. All the complexes show an efficient binding interaction towards BSA and we found that the binding constants are in the order of **4** > **1** > **3** > **5** > **2**. In addition, antiproliferative activity of **1–5** against the A549 cancer cell line has been examined by using MTT assay. Complex **2** was the most cytotoxic against A549, while propidium iodide staining assay revealed dose dependent cell death for all the complexes. The results of the present study regarding the abilities of new oxidovanadium(IV) complexes further inspire us to continue on with the development of metal-based agents for anti-cancer studies.

Conflicts of interest

There are no conflicts to declare.

Acknowledgements

R. D. thanks DBT, Govt. of India [Grant No. 6242-P112/RGCB/PMD/DBT/RPDA/2015] and CSIR, Govt. of India [Grant No. 01(2963)/18/EMR-II] for funding this research. E. G. thanks Fondazione di Sardegna (project FDS15Garribba) and Regione Autonoma della Sardegna (grant RASSR79857) for the financial support.

References

1 (*a*) L. Kelland, *Nat. Rev. Cancer*, 2007, **7**, 573; (*b*) G. Sava, G. Jaouen, E. A. Hillard and A. Bergamo, *Dalton Trans.*, 2012, **41**, 8226; (*c*) C. G. Hartinger, N. Metzler-Nolte and P. J. Dyson, *Organometallics*, 2012, **31**, 5677; (*d*) N. P. Barry and P. J. Sadler, *Chem. Commun.*, 2013, **49**, 5106; (*e*) K. R. Barnes and S. J. Lippard*Metal Complexes in Tumor Diagnosis and as Anticancer Agents*, Marcel Dekker, New York/Basel, 2004, vol. 42, p. 179; (*f*) H. Zhang, L. Guo, Z. Tian, M. Tian, S. Zhang, Z. Xu, P. Gong, X. Zheng, J. Zhaoa and Z. Liu, *Chem. Commun.*, 2018, **54**, 4421; (*g*) C. H. Leung, H. J. Zhong, D. S. H. Chan and D. L. Ma, *Coord. Chem. Rev.*, 2013, **257**, 1764; (*h*) Y. Jung and S. J. Lippard, *Chem. Rev.*, 2007, **107**, 1387; (*i*) E. R. Jamieson and S. J. Lippard, *Chem. Rev.*, 1999, **99**, 2467.

2 (*a*) E. Alessio, G. Mestroni, A. Bergamo and G. Sava, Metal ions in Biological Systems, in *Metal Complexes in Tumor Diagnosis and as Anticancer Agents*, ed. A. Sigel and H. Sigel, Marcel Dekker Inc., New York, 2004, vol. 42, p. 323;

(*b*) A. P. Carnizello, M. I. F. Barbosa, M. Martins, N. H. Ferreira, P. F. Oliveira, G. M. Magalhaes, A. A. Batista and D. C. Tavares, *J. Inorg. Biochem.*, 2016, **164**, 42; (*c*) E. Meggers, *Angew. Chem., Int. Ed.*, 2011, **50**, 2442; (*d*) C. G. Hartinger, M. A. Jakupec, S. Zorbas-Seifried, M. Groessl, A. Egger, W. Berger, H. Zorbas, P. J. Dyson and B. K. Keppler, *Chem. Biodiversity*, 2008, **5**, 2140.

3 (*a*) K. E. Erkkila, D. T. Odom and J. K. Barton, *Chem. Rev.*, 1999, **99**, 2777; (*b*) M. Manosas, J. Camunas-Soler, V. Croquette and F. Ritort, *Nat. Commun.*, 2017, **8**, 304; (*c*) Y. Xiong and L. N. Ji, *Coord. Chem. Rev.*, 1999, **185**, 711; (*d*) D. S. Sigman, A. Mazumder and D. M. Perrin, *Chem. Rev.*, 1993, **93**, 2295; (*e*) E. M. Boon, J. K. Barton, P. I. Pradeepkumar, J. Isaksson, C. Petit and J. Chattopadhyaya, *Angew. Chem., Int. Ed.*, 2002, **41**, 3402; (*f*) C. Metcalfe and J. A. Thomas, *Chem. Soc. Rev.*, 2003, **32**, 215.

4 (*a*) S.-L. Zhang, G. L. V. Damu, L. Zhang, R.-X. Geng and C.-H. Zhou, *Eur. J. Med. Chem.*, 2012, **55**, 164; (*b*) X. M. He and D. C. Carter, *Nature*, 1992, **358**, 209; (*c*) T. Banerjee, S. K. Singh and N. Kishore, *J. Phys. Chem. B*, 2006, **110**, 24147.

5 (*a*) V. G. Sankareswari, D. Vinod, A. Mahalakshmi, M. Alamelu, G. Kumaresan, R. Ramaraj and S. Rajagopal, *Dalton Trans.*, 2014, **43**, 3260; (*b*) Z. G. Yasseen, *J. Chem. Pharm. Res.*, 2012, **4**, 3361; (*c*) P. Krishnamoorthy, P. Sathyadevi, A. H. Cowley, R. R. Butorac and N. Dharmaraj, *Eur. J. Med. Chem.*, 2011, **46**, 3376; (*d*) D. Sanna, L. Biro, P. Buglyo, G. Micera and E. Garribba, *Metallomics*, 2012, **4**, 33.

6 (*a*) P. Sathyadevi, P. Krishnamoorthy, R. R. Butorac, A. H. Cowley, N. S. P. Bhuvanesh and N. Dharmaraj, *Dalton Trans.*, 2011, **40**, 9690; (*b*) V. C. Silveira, M. P. Abbott, M. Cavicchioli, M. B. Goncalves, H. M. Petrilli, L. de Rezende, A. T. Amaral, D. E. P. Fonseca, G. F. Caramori and A. M. da Costa Ferreira, *Dalton Trans.*, 2013, 6386; (*c*) A. Patra, T. K. Sen, A. Ghorai, G. T. Musie, S. K. Mandal, U. Ghosh and M. Bera, *Inorg. Chem.*, 2013, **52**, 2880; (*d*) X.-W. Li, L. Tao, Y.-T. Li, Z.-Y. Wu and C.-W. Yan, *Eur. J. Med. Chem.*, 2012, **54**, 697; (*e*) M. A. Neelakantan, C. Balakrishnan, V. Selvarani and M. Theetharappan, *Appl. Organomet. Chem.*, 2018, **32**, e4125; (*f*) N.-u. H. Khan, N. Pandya, N. C. Maity, M. Kumar, R. M. Patel, R. I. Kureshy, S. H. R. Abdi, S. Mishra, S. Das and H. C. Bajaj, *Eur. J. Med. Chem.*, 2011, **46**, 5074; (*g*) M. W. Makinen and M. Salehitazangi, *Coord. Chem. Rev.*, 2014, **279**, 1; (*h*) B. Mukherjee, B. Patra, S. Mahapatra, P. Banerjee, A. Tiwari and M. Chatterjee, *Toxicol. Lett.*, 2004, **150**, 135.

7 (*a*) S. P. Dash, S. Pasayat, S. Bhakat, S. Roy, R. Dinda, E. R. T. Tiekink, S. Mukhopadhyay, S. K. Bhutia, M. R. Hardikar, B. N. Joshi, Y. P. Patil and M. Nethaji, *Inorg. Chem.*, 2013, **52**, 14096; (*b*) S. P. Dash, A. K. Panda, S. Pasayat, R. Dinda, A. Biswas, E. R. T. Tiekink, Y. P. Patil, M. Nethaji, W. Kaminsky, S. Mukhopadhyay and S. K. Bhutia, *Dalton Trans.*, 2014, **43**, 10139; (*c*) S. P. Dash, A. K. Panda, S. Pasayat, R. Dinda, A. Biswas, E. R. T. Tiekink, S. Mukhopadhyay, S. K. Bhutia, W. Kaminsky and E. Sinn, *RSC Adv.*, 2015, **5**, 51852; (*d*) S. P. Dash, A. K. Panda, S. Pasayat, S. Majumder, A. Biswas, W. Kaminsky, S. Mukhopadhyay, S. K. Bhutia and R. Dinda, *J. Inorg. Biochem.*, 2015, **144**, 1; (*e*) S. P. Dash, A. K. Panda, S. Dhaka, S. Pasayat, A. Biswas, M. R. Maurya, P. K. Majhi, A. Crochet and R. Dinda, *Dalton Trans.*, 2016, **45**, 18292; (*f*) Saswati, P. Adão, S. Majumder, S. P. Dash, S. Roy, M. L. Kuznetsov, J. Costa Pessoa, C. S. B. Gomes, M. R. Hardikar, E. R. T. Tiekink and R. Dinda, *Dalton Trans.*, 2018, **47**, 11358; (*g*) S. Roy, M. Bohme, A. Buchholz, W. Plass, S. P. Dash, M. Mohanty, S. Majumder, S. Kulanthaivel, I. Banerjee and R. Dinda, *Inorg. Chem.*, 2018, **57**, 5767; (*h*) S. P. Dash, S. Pasayat, Saswati, H. R. Dash, S. Das, R. J. Butcher and R. Dinda, *Polyhedron*, 2012, **31**, 524.

8 (*a*) T. Yamaguchi, S. Watanabe, Y. Matsumura, Y. Tokuoka and A. Yokoyama, *Bioorg. Med. Chem.*, 2012, **20**, 3058; (*b*) M. J. Xie, Y. F. Niu, X. D. Yang, W. P. Liu, L. Li, L. H. Gao, S. P. Yan and Z. H. Meng, *Eur. J. Med. Chem.*, 2010, **45**, 6077; (*c*) J. C. Pessoa, S. Etcheverry and D. Gambino, *Coord. Chem. Rev.*, 2015, **301**, 24; (*d*) E. Kioseoglou, S. Petanidis, C. Gabriel and A. Salifoglou, *Coord. Chem. Rev.*, 2015, **301**, 87.

9 I. Correia, S. Roy, C. P. Matos, S. Borovic, N. Butenko, I. Cavaco, F. Marques, J. Lorenzo, A. Rodríguez, V. Moreno and J. C. Pessoa, *J. Inorg. Biochem.*, 2015, **147**, 134.

10 L. Andrezálová, H. Gbelcová and Z. Ďuračková, *J. Trace Elem. Med. Biol.*, 2013, **27**, 21.

11 (*a*) P. Noblía, E. J. Baran, L. Otero, P. Draper, H. Cerecetto, M. González, O. E. Piro, E. E. Castellano, T. Inohara, Y. Adachi, H. Sakurai and D. Gambino, *Eur. J. Inorg. Chem.*, 2004, 322; (*b*) K. H. Thompson, J. H. McNeill and C. Orvig, *Chem. Rev.*, 1999, **99**, 2561; (*c*) T. Jakusch and T. Kiss, *Coord. Chem. Rev.*, 2017, **351**, 118; (*d*) Y. Shechter and S. J. D. Karlish, *Nature*, 1980, **284**, 556; (*e*) C. E. Heyliger, A. G. Tahiliani and J. H. McNeill, *Science*, 1985, **227**, 1474; (*f*) S. Ramanadham, J. J. Mongold, R. W. Brownsey, G. H. Cros and J. H. McNeill, *Am. J. Physiol.*, 1989, **257**, H904; (*g*) J. H. McNeill, V. G. Yuen, H. R. Hoveyda and C. Orvig, *J. Med. Chem.*, 1992, **35**, 1489; (*h*) Y. Schecter, J. Meyerovitch, Z. Farfel, J. Sack, S. Bar-Meir, S. Amir, H. Degani and S. J. D. Karlish, *Vanadium in Biological Systems*, Kluwer Academic Publishers, Norwell, MA, 1990, p. 129; (*i*) K. H. Thompson, J. H. McNeill and C. Orvig, *Topics in Biological Chemistry: Metallopharmaceuticals*, Springer-Verlag, Heidelberg, 1999, vol. 2, p. 139.

12 J. Pranczk, D. Jacewicz, D. Wyrzykowski, A. Wojtczak, A. Tesmar and L. Chmurzyński, *Eur. J. Inorg. Chem.*, 2015, 3343.

13 M. Weyand, H. J. Hecht, M. Kieß, M. F. Liaud, H. Vitler and D. Schomburg, *J. Mol. Biol.*, 1999, **293**, 595.

14 (*a*) W. Plass, *Angew. Chem., Int. Ed.*, 1999, **38**, 909; (*b*) A. Butler and J. V. Walker, *Chem. Rev.*, 1993, **93**, 1937.

15 J. N. Carter-Franklin, J. D. Parrish, R. A. Tchirret-Guth, R. D. Little and A. Butler, *J. Am. Chem. Soc.*, 2003, **125**, 3688.

16 D. Rehder, G. Antoni, G. M. Licini, C. Schulzke and B. Meier, *Coord. Chem. Rev.*, 2003, **237**, 53.

17 (*a*) D. C. Crans, R. A. Felty and M. M. Miller, *J. Am. Chem. Soc.*, 1991, **113**, 265; (*b*) F. Hillerns, F. Olbrich, U. Behrens and D. Rehder, *Angew. Chem., Int. Ed. Engl.*, 1992, **31**, 447.

18 (*a*) R. R. Eady, *Coord. Chem. Rev.*, 2003, **237**, 23; (*b*) D. Rehder, *Dalton Trans.*, 2013, **42**, 11749.
19 (*a*) J. C. Pessoa, S. Etcheverry and D. Gambino, *Coord. Chem. Rev.*, 2015, **301–302**, 24; (*b*) D. Gambino, *Coord. Chem. Rev.*, 2011, **255**, 2193.
20 (*a*) B. Sarkar, S. Patra, J. Fiedler, R. B. Sunoj, D. Janardanan, G. K. Lahiri and W. Kaim, *J. Am. Chem. Soc.*, 2008, **130**, 3532; (*b*) B. Sarkar, S. Patra, J. Fiedler, R. B. Sunoj, D. Janardanan, S. M. Mobin, M. Niemeyer, G. K. Lahiri and W. Kaim, *Angew. Chem., Int. Ed.*, 2005, **44**, 5655.
21 S. Samanta, P. Ghosh and S. Goswami, *Dalton Trans.*, 2012, **41**, 2213.
22 (*a*) S. Kawata and Y. Kawata, *Chem. Rev.*, 2000, **100**, 1777; (*b*) A. Bianchi, E. Delgado-Pinar, E. García-España, C. Giorgi and F. Pina, *Coord. Chem. Rev.*, 2014, **260**, 156; (*c*) W. Kaim, *Coord. Chem. Rev.*, 2001, **219**, 463; (*d*) G. Pourrieux, F. Fagalde, I. Romero, X. Fontrodona, T. Parella and N. E. Katz, *Inorg. Chem.*, 2010, **49**, 4084; (*e*) A. Sanyal, P. Banerjee, G.-H. Lee, S.-M. Peng, C.-H. Hung and S. Goswami, *Inorg. Chem.*, 2004, **43**, 7456; (*f*) N. M. Aljamali, *Biochem. Anal. Biochem.*, 2015, **4**, 169.
23 K. Nejati, Z. Rezvani and M. Seyedahmadian, *Dyes Pigm.*, 2009, **83**, 304.
24 (*a*) C. Kaes, A. Katz and M. W. Hosseini, *Chem. Rev.*, 2000, **100**, 3553; (*b*) A. Bencini and V. Lippolis, *Coord. Chem. Rev.*, 2010, **254**, 2096; (*c*) R. P. Thummel, in *Comprehensive Coordination Chemistry II*, ed. J. A. McCleverty and T. J. Mayer, Elsevier, Oxford, 2004, vol. 1, p. 41.
25 J. H. Thurston, E. M. Marlier and K. H. Whitmire, *Chem. Commun.*, 2002, 2834.
26 (*a*) O. Novakova, J. Kasparkova, O. Vrana, P. M. van Vliet, J. Reedijk and V. Brabec, *Biochemistry*, 1995, **34**, 12369; (*b*) J. Costa Pessoa and I. Tomaz, *Curr. Med. Chem.*, 2010, **17**, 3701 and references therein.
27 (*a*) F. P. Pruchnik, M. Bień and T. Lachowicz, *Met.-Based Drugs*, 1996, **3**, 185; (*b*) M. Bień, T. M. Lachowicz, A. Rybka, F. P. Pruchnik and L. Trynda, *Met.-Based Drugs*, 1997, **4**, 81; (*c*) M. Bień, F. P. Pruchnik, A. Seniuk, T. M. Lachowicz and P. Jakimowicz, *J. Inorg. Biochem.*, 1999, **73**, 49.
28 (*a*) H. Mansuri-Torshizi, T. S. Srivastava, H. K. Parekh and M. P. Chitnis, *J. Inorg. Biochem.*, 1992, **45**, 135; (*b*) G. Zhao and H. Lin, *Curr. Med. Chem.*, 2005, **5**, 137.
29 (*a*) I. Ott, *Coord. Chem. Rev.*, 2009, **253**, 1670; (*b*) A. Bindoli, M. P. Rigobello, G. Scutari, C. Gabbiani, A. Casini and L. Messori, *Coord. Chem. Rev.*, 2009, **253**, 1692.
30 E. Meléndez, *Crit. Rev. Oncol. Hematol.*, 2002, **42**, 309.
31 A. Valentini, F. Conforti, A. Crispini, A. De Martino, R. Condello, C. Stellitano, G. Rotilio, M. Ghedini, G. Federici, S. Bernardini and D. Pucci, *J. Med. Chem.*, 2009, **52**, 484.
32 A. Kellett, M. O'Connor, M. McCann, O. Howe, A. Casey, P. McCarron, K. Kavanagh, M. McNamara, S. Kennedy, D. D. May, P. S. Skell, D. O'Shea and M. Devereux, *Med. Chem. Commun.*, 2011, **2**, 579.
33 (*a*) R. K. Narla, Y. Dong, O. J. D'Cruz, C. Navara and F. M. Uckun, *Clin. Cancer Res.*, 2000, **6**, 1546; (*b*) R. K. Narla, C.-L. Chen, Y. Dong and F. M. Uckun, *Clin. Cancer Res.*, 2001, **7**, 2124; (*c*) O. J. D'Cruz and F. M. Uckun, *Expert Opin. Invest. Drugs*, 2002, **11**, 1829.
34 A. M. Kordowiak, W. Dabroś and B. Kojda, *Horm. Metab. Res.*, 2002, **34**, 556.
35 R. Francik, M. Krósniak, M. Barlik, A. Kudła, R. Gryboś and T. Librowski, *Bioinorg. Chem. Appl.*, 2011, 206316.
36 (*a*) D. C. Crans, J. J. Smee, E. Gaidamauskas and L. Yang, *Chem. Rev.*, 2004, **104**, 849; (*b*) D. Rehder, *Bioinorganic Vanadium Chemistry*, Wiley, Chichester, 2008; (*c*) D. Sanna, P. Buglyo, A. I. Tomaz, J. C. Pessoa, S. Borovic, G. Micera and E. Garribba, *Dalton Trans.*, 2012, **41**, 12824.
37 (*a*) S. Pasayat, M. Böhme, S. Dhaka, S. P. Dash, S. Majumder, M. R. Maurya, W. Plass, W. Kaminsky and R. Dinda, *Eur. J. Inorg. Chem.*, 2016, 1604; (*b*) S. P. Dash, S. Roy, M. Mohanty, M. F. N. N. Carvalho, M. L. Kuznetsov, J. Costa Pessoa, A. Kumar, Y. P. Patil, A. Crochet and R. Dinda, *Inorg. Chem.*, 2016, **55**, 8407; (*c*) S. P. Dash, S. Majumder, A. Banerjee, M. F. N. N. Carvalho, P. Adão, J. C. Pessoa, K. Brzezinski, E. Garribba, H. Reuter and R. Dinda, *Inorg. Chem.*, 2016, **55**, 1165; (*d*) R. Dinda, P. K. Majhi, P. Sengupta, S. Pasayat, S. Ghosh, L. R. Falvello and T. C. W. Mak, *Polyhedron*, 2010, **29**, 248.
38 R. A. Rowe and M. Jones, *Inorg. Synth.*, 1957, **5**, 113.
39 *WINEPR SimFonia, version 1.25*, Bruker Analytische Messtechnik GmbH, Karlshrue, 1996.
40 Bruker (2007) *APEX2 (Version 2.1-4), SAINT (version 7.34A), SADABS (version 2007/4)*, BrukerAXS Inc, Madison, Wisconsin, USA.
41 (*a*) A. Altomare, C. Burla, M. Camalli, G. L. Cascarano, C. Giacovazzo, A. Guagliardi, A. G. G. Moliterni, G. Polidori and R. Spagna, *J. Appl. Crystallogr.*, 1999, **32**, 115; (*b*) A. Altomare, G. L. Cascarano, C. Giacovazzo and A. Guagliardi, *J. Appl. Crystallogr.*, 1993, **26**, 343.
42 G. M. Sheldrick, *Acta Crystallogr., Sect. A: Found. Adv.*, 2015, **71**, 3.
43 (*a*) G. M. Sheldrick, *SHELXL-97, Program for the Refinement of Crystal Structures*, University of Göttingen, Germany, 1997; (*b*) G. M. Sheldrick, *Acta Crystallogr., Sect. C: Struct. Chem.*, 2015, **71**, 3.
44 S. Mackay, C. Edwards, A. Henderson, C. Gilmore, N. Stewart, K. Shankland and A. Donald, *MaXus: a computer program for the solution and refinement of crystal structures from diffraction data*, University of Glasgow, Scotland, 1997.
45 D. Waasmaier and A. Kirfel, *Acta Crystallogr., Sect. A: Found. Crystallogr.*, 1995, **51**, 416.
46 M. J. Frisch, G. W. Trucks, H. B. Schlegel, G. E. Scuseria, M. A. Robb, J. R. Cheeseman, G. Scalmani, V. Barone, B. Mennucci, G. A. Petersson, H. Nakatsuji, M. L. Caricato, H. P. Hratchian, A. F. Izmaylov, J. Bloino, G. Zheng, J. L. Sonnenberg, M. Hada, M. Ehara, K. Toyota, R. Fukuda, J. Hasegawa, M. Ishida, T. Nakajima, Y. Honda, O. Kitao, H. Nakai, T. Vreven, J. A. Montgomery Jr., J. E. Peralta, F. Ogliaro, M. Bearpark, J. J. Heyd, E. Brothers, K. N. Kudin, V. N. Staroverov, T. Keith, R. Kobayashi, J. Normand, K. Raghavachari, A. Rendell, J. C. Burant, S. S. Iyengar,

J. Tomasi, M. Cossi, N. Rega, J. M. Millam, M. Klene, J. E. Knox, J. B. Cross, V. Bakken, C. J. Adamo, R. Gomperts, R. E. Stratmann, O. Yazyev, A. J. Austin, R. Cammi, C. Pomelli, J. W. Ochterski, R. L. Martin, K. Morokuma, V. G. Zakrzewski, G. A. Voth, P. Salvador, J. J. Dannenberg, S. Dapprich, A. D. Daniels, Ö. Farkas, J. B. Foresman, J. V. Ortiz, J. Cioslowski and D. J. Fox, *Gaussian 09, revision D.01*, Gaussian, Inc., Wallingford, CT, 2010.

47 (*a*) G. Micera and E. Garribba, *Int. J. Quantum Chem.*, 2012, **112**, 2486; (*b*) L. Pisano, K. Varnagy, S. Timári, K. Hegetschweiler, G. Micera and E. Garribba, *Inorg. Chem.*, 2013, **52**, 5260; (*c*) D. Sanna, K. Várnagy, N. Lihi, G. Micera and E. Garribba, *Inorg. Chem.*, 2013, **52**, 8202.

48 (*a*) G. Micera and E. Garribba, *Eur. J. Inorg. Chem.*, 2010, 4697; (*b*) D. Sanna, K. Varnágy, S. Timári, G. Micera and E. Garribba, *Inorg. Chem.*, 2011, **50**, 10328; (*c*) S. Kundu, D. Mondal, K. Bhattacharya, A. Endo, D. Sanna, E. Garribba and M. Chaudhury, *Inorg. Chem.*, 2015, **54**, 6203; (*d*) D. Sanna, V. Ugone, G. Micera, P. Buglyo, L. Biro and E. Garribba, *Dalton Trans.*, 2017, **46**, 8950.

49 (*a*) G. Micera and E. Garribba, *J. Comput. Chem.*, 2011, **32**, 2822; (*b*) D. Sanna, V. Pecoraro, G. Micera and E. Garribba, *J. Biol. Inorg. Chem.*, 2012, **17**, 773; (*c*) D. Sanna, G. Sciortino, V. Ugone, G. Micera and E. Garribba, *Inorg. Chem.*, 2016, **55**, 7373.

50 N. F. Choudhary, N. G. Connelly, P. B. Hitchcock and G. J. Leigh, *J. Chem. Soc., Dalton Trans.*, 1999, 4437.

51 (*a*) J. Selbin, *Coord. Chem. Rev.*, 1966, **1**, 293; (*b*) A. Syamal, *Transition Met. Chem.*, 1978, **3**, 259.

52 S. Dutta, P. Basu and A. Chakravorty, *Inorg. Chem.*, 1993, **32**, 5343.

53 E. Garribba and G. Micera, *J. Chem. Educ.*, 2006, **83**, 1229.

54 A. C. Rizzi, N. I. Neuman, P. J. González and C. D. Brondino, *Eur. J. Inorg. Chem.*, 2016, 192.

55 P. K. Sasmal, A. K. Patra and A. R. Chakravarty, *J. Inorg. Biochem.*, 2008, **102**, 1463.

56 J. Chakravarty, S. Dutta, S. K. Chandra, P. Basu and A. Chakravorty, *Inorg. Chem.*, 1993, **32**, 4249.

57 F. Arjmand, B. Mohani and S. Ahmad, *Eur. J. Med. Chem.*, 2005, **40**, 1103.

58 F. Arjmand and M. Aziz, *Eur. J. Med. Chem.*, 2009, **44**, 834.

59 E. Gao, L. Liu, M. Zhu, Y. Huang, F. Guan, X. Gao, M. Zhang, L. Wang, W. Zhang and Y. Sun, *Inorg. Chem.*, 2011, **50**, 4732.

60 P. J. Bindu, K. M. Mahadevan, T. R. R. Naik and B. G. Harish, *Med. Chem. Commun.*, 2014, **5**, 1708.

61 M. Sirajuddin, S. Ali and A. Badshah, *J. Photochem. Photobiol., B*, 2013, **124**, 1.

62 Y. Sun, Y.-J. Hou, Q.-X. Zhou, W.-H. Lei, J.-R. Chen, X.-S. Wang and B.-W. Zhang, *Inorg. Chem.*, 2010, **49**, 10108.

63 Z.-G. Wang, Y.-Y. Kou, J. Lu, C.-Y. Gao, J.-L. Tian and S.-P. Yan, *Appl. Organomet. Chem.*, 2012, **26**, 511.

64 S. Chatterjee and T. K. Mukherjee, *Phys. Chem. Chem. Phys.*, 2014, **16**, 8400.

65 S. Saha, R. Majumdar, M. Roy, R. R. Dighe and A. R. Chakravarty, *Inorg. Chem.*, 2009, **48**, 2652.

66 N. Pradhan, S. Parbin, S. Kar, L. Das, R. Kirtana, G. S. Seshadri, D. Sengupta, M. Deb, C. Kausar and S. K. Patra, *Biochim. Biophys. Acta, Mol. Basis Dis.*, 2019, **1865**, 1651.

67 S. Parbin, N. Pradhan, L. Das, P. Saha, M. Deb, D. Sengupta and S. K. Patra, *Exp. Cell Res.*, 2019, **374**, 323.

68 G. Y. Park, J. J. Wilson, Y. Song and S. J. Lippard, *Proc. Natl. Acad. Sci. U. S. A.*, 2012, **109**, 11987.

69 S. Majumder, S. Pasayat, A. K. Panda, S. P. Dash, S. Roy, A. Biswas, M. E. Varma, B. N. Joshi, E. Garribba, C. Kausar, S. K. Patra, W. Kaminsky, A. Crochet and R. Dinda, *Inorg. Chem.*, 2017, **56**, 11190.

70 L. C. Crowley, A. P. Scott, B. J. Marfell, J. A. Boughaba, G. Chojnowski and N. J. Waterhouse, *Cold Spring Harb. Protoc.*, 2016, DOI: 10.1101/pdb.prot08716.